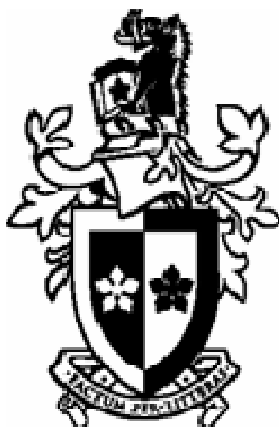


COMPUTATIONAL SIMULATION OF HYPERBRANCHED POLYMER MELTS UNDER SHEAR



Tu Cam Le

*Dissertation
submitted in fulfilment of requirements for the degree of
Doctor of Philosophy*

Centre for Molecular Simulation

**Faculty of Information and Communication Technologies
Swinburne University of Technology**

2010

Abstract

In this work, hyperbranched polymers of different molecular weights and different molecular architectures have been simulated using a coarse-grained model and non-equilibrium molecular dynamics techniques. A number of structural parameters and the rheology of hyperbranched polymer melts under shear were analysed to explain the effect of the molecular structure and molecular weight on microscopic as well as macroscopic properties.

In order to determine the shear-induced changes in the structural properties of hyperbranched polymers, various parameters were calculated at different strain rates. The radii of gyration which characterize the size of the polymer were evaluated. The relationship between the zero shear rate mean squared radius of gyration and the molecular weight as well as the Wiener index was established. The tensor of gyration was analysed and results indicate that hyperbranched polymer molecules have a prolate ellipsoid shape under shear. As hyperbranched polymers have compact, highly branched architecture and layers of beads have increasing densities which might lead to an unusual distribution of mass, the distribution of beads was also studied. The distribution of terminal beads was investigated to understand the spatial arrangement of these groups which is very important for hyperbranched polymer applications, especially in drug delivery. Flow birefringence was characterized by taking into account both form and intrinsic birefringences which result from molecular and bond alignment respectively.

The melt rheology of hyperbranched polymer structures with different molecular weights and different number of spacers was also studied. Systems were simulated over a wide range of strain rates to capture the crossover behaviour from Newtonian to non-Newtonian regimes. Rheological properties including the shear viscosity and first and second normal stress coefficients were computed and the transition to shear thinning was observed at different strain rates for hyperbranched polymers of different sizes and topologies. The results were consistent with findings from NEMD simulations of linear and dendritic polymers. The stress-optical rule was tested and shown to be valid only in the Newtonian regime and violated in the strong flow regime where the rule does not

take into account flow-induced changes of the micro structure. The stress-optical coefficient was found to be independent of the molecular weight and topology of polymers.

Blends of hyperbranched polymers and linear polymers were also simulated and their rheological properties were investigated. Results show that even a small proportion of hyperbranched polymer in a melt of linear chains can reduce the shear viscosity of the whole system. This feature makes hyperbranched polymers a potential candidate as rheology modifiers. However there is no observed limit in the proportion of hyperbranched polymers in the samples above which the viscosity is stabilized. The viscosity drops continuously, correlating with the amount of hyperbranched polymers present.

Acknowledgements

I would like to sincerely acknowledge Prof. Billy D. Todd, A/Prof. Peter J. Davis and Dr. Alfred Uhlherr for their great supervision during my study at the Centre for Molecular Simulation, Swinburne University of Technology. They have given me guidance, inspiring suggestions, and encouragement at every stage of my work. I appreciate the opportunity of working with them and learning from them.

I would like to thank to Swinburne University of Technology and Swinburne Research in particular for financial support through an International Postgraduate Research Scholarship and the Faculty of Information and Communication Technologies for supporting my workshop and conference experience. I am indebted to the university for providing the great infrastructure especially library resources and supercomputer facilities for my study.

I am grateful to Dr. Jaroslaw Bosko, Dr. Jesper Hansen and Dr. Alexe Bojovschi for constructive suggestions and valuable advice which greatly improved the progress of this work.

I am thankful to all staff and students of the Centre for Molecular Simulation for a friendly environment, encouraging discussions and all the social activities that we had together.

Thanks to all my friends from the Explorers Club with whom I have had a great time discovering beautiful Victoria and learnt more about the multi-cultural Australia.

Finally, my deepest thanks to my family for their endless love, support and encouragement for every step I make in my life.

Declaration

I hereby declare that the thesis entitled “Computational simulation of hyperbranched polymer melts under shear”, and submitted in fulfilment of the requirements for the Degree of Doctor of Philosophy in the Faculty of Information and Communication Technologies of Swinburne University of Technology, is my own work and that it contains no material which has been accepted for the award to the candidate of any other degree or diploma, except where due reference is made in the text of the thesis. To the best of my knowledge and belief, it contains no material previously published or written by another person except where due reference is made in the text of the thesis.

Tu Cam Le

December 2009

Publications from this thesis

The following papers have been based on part of this work:

1. Tu C. Le, Billy D. Todd, Peter J. Daivis, Alfred Uhlherr (2008), “*Rheology and Structural Properties of Hyperbranched Polymers: a Non-Equilibrium Molecular Dynamics Study*”, The XVth International Congress on Rheology, published by the American Institute of Physics, **1027**, ISBN 978-0-7354-0549-3, pp433
2. Tu C. Le, B. D. Todd, P. J. Daivis and A. Uhlherr (2009) “*Structural properties of hyperbranched polymers in the melt under shear via non-equilibrium molecular dynamics simulation*”, Journal of Chemical Physics, **130**, 074901
3. Tu C. Le, B. D. Todd, P. J. Daivis and A. Uhlherr (2009) “*Rheology of hyperbranched polymer melts undergoing planar Couette flow*”, Journal of Chemical Physics, **131**, 044902
4. Tu C. Le, B. D. Todd, P. J. Daivis and A. Uhlherr (2009) “*The effect of inter-branch spacing on structural and rheological properties of hyperbranched polymers*”, Journal of Chemical Physics, **131**, 164901
5. Tu C. Le, B. D. Todd, P. J. Daivis and A. Uhlherr “*The effect of adding hyperbranched polymers in linear polymers melts on structural and rheological properties of blend systems*”, (in preparation)

Table of Contents

Abstract	<i>i</i>
Acknowledgements	<i>iii</i>
Declaration	<i>iv</i>
Publications from this thesis	<i>v</i>
Table of Contents	<i>vi</i>
Table of Figures	<i>ix</i>
List of Tables	<i>xv</i>
Notation	<i>xvii</i>
1. GENERAL INTRODUCTION	1
2. HYPERBRANCHED POLYMERS	4
2.1. Topology	4
2.2. History and synthesis methodology	5
2.3. Properties	7
2.4. Theoretical models	8
2.5. Applications	10
3. STRUCTURE AND RHEOLOGY OF POLYMERIC FLUIDS	12
3.1. Structural properties of polymers	12
3.1.1. Degree of branching and Wiener index	12
3.1.2. Radius of gyration	14
3.1.3. Radial distribution of mass	14
3.2. Flow birefringence	15
3.3. Rheology of polymeric fluids	16
3.3.1. Shear stress	18
3.3.2. Non-Newtonian viscosity	19
3.3.3. Normal stress effects	19
3.3.4. Dimensionless groups in non-Newtonian fluid mechanics	20

4. MOLECULAR DYNAMICS SIMULATION.....	22
4.1. Brief overview of different computer simulation methods.....	22
4.2. Coarse-grained model	23
4.3. Intermolecular interaction	26
4.4. Periodic boundary conditions.....	29
4.5. Equations of motion	31
4.6. Integration	36
4.7. Simulation conditions	39
5. STRUCTURAL PROPERTIES OF HYPERBRANCHED POLYMERS	41
5.1. Conformation of simulated hyperbranched polymers.....	41
5.2. Radius of gyration	48
5.2.1. <i>Radius of gyration of hyperbranched polymers with different molecular weights.....</i>	<i>48</i>
5.2.2. <i>Radius of gyration of hyperbranched polymers with different numbers of spacers</i>	<i>51</i>
5.2.3. <i>Radius of gyration of the blends composed of hyperbranched polymers and linear chains of equivalent molecular weight</i>	<i>55</i>
5.3. Tensor of gyration.....	57
5.4. Distribution of mass	62
5.4.1. <i>Distribution of mass for hyperbranched polymers of different molecular weights</i>	<i>62</i>
5.4.2. <i>Distribution of mass for hyperbranched polymers with the same molecular weight of 187 beads but different numbers of spacers</i>	<i>65</i>
5.4.3. <i>Distribution of mass for blends of hyperbranched polymers and linear polymers of the equivalent molecular weight.....</i>	<i>68</i>
5.5. Distribution of terminal groups.....	71
5.6. Atomic radial distribution function.....	71
5.7. Interpenetration	74
5.7.1. <i>Interpenetration function for hyperbranched polymers of different molecular weights</i>	<i>74</i>
5.7.2. <i>Interpenetration function for hyperbranched polymers with different numbers of spacers.....</i>	<i>76</i>

5.8. Flow birefringence	77
5.8.1. Form birefringence.....	77
5.8.2. Intrinsic birefringence	82
6. RHEOLOGY OF HYPERBRANCHED POLYMER MELTS.....	89
6.1. Introduction.....	89
6.2. Shear viscosity	90
6.2.1. Shear viscosity for hyperbranched polymers of different molecular weights	90
6.2.2. Shear viscosities for hyperbranched polymers with different numbers of spacers	96
6.2.3. Shear viscosity of hyperbranched polymer blends	103
6.3. First and second normal stress coefficients.....	109
6.3.1. Normal stress coefficients for hyperbranched polymers of different molecular weights	110
6.3.2. Normal stress coefficients of hyperbranched polymers with different numbers of spacers	113
6.3.3. Normal stress coefficients of hyperbranched polymer blends.....	116
6.4. Pressure and density	119
6.4.1. Pressure of hyperbranched polymers of different molecular weights.....	119
6.4.2. Pressure and density of hyperbranched polymers with different numbers of spacers	121
6.4.3. Density of blends of hyperbranched and linear polymers	124
6.5. Stress-optical rule.....	126
6.5.1. Stress-optical rule for hyperbranched polymers of different molecular weights.....	126
6.5.2. Stress-optical rule for hyperbranched polymers with different number of spacers	128
7. CONCLUSIONS	130
REFERENCES	134

Table of Figures

Figure 1.1. Configuration of different branched polymers. (a) Graft (b) Star (c) Comb and (d) Dendritic polymers.	1
Figure 1.2. Comparison between the architecture of a dendrimer molecule and a randomly branched hyperbranched polymer molecule.	2
Figure 1.3. The number of scientific publications as a function of publication year based on a search by ISI web of science with hyperbranched polymers as the topic.	2
Figure 2.1. Schematic configuration of a tri-functional dendrimer of generation 3 and an example of a hyperbranched polymer molecule.	4
Figure 3.1. Degree of branching for different polymer architectures of the same molecular weight (blue beads representing linear units and red beads representing branching units).....	13
Figure 3.2. Wiener index for different polymer architectures of the same molecular weight (10 monomers).	13
Figure 3.3. Simple geometries for producing shear flows (a) sliding plates (planar Couette geometry), (b) concentric cylinders (cylindrical Couette geometry), (c) parallel disks or plate-and-plate (torsional flow) and (d) the cone-and-plate. (adopted from (Macosko, 1994)).	17
Figure 3.4. Streaming velocity profile of the polymeric fluid undergoing planar Couette flow.	18
Figure 4.1. The first coarse-grained models – the rigid and elastic dumbbell models. ...	24
Figure 4.2. The freely jointed bead-rod and bead-spring chain models.....	25
Figure 4.3. Interaction potential between non-bonded beads which interact via only the WCA potential and bonded beads which interact via both WCA and FENE potential.....	28
Figure 4.4. Periodic boundary condition in two dimensions with the primary cell surrounded by its image cells. Molecules that leave the cell will be replaced by their images entering the cell from the opposite side.....	30
Figure 4.5. Lees-Edwards periodic boundary conditions for steady shear.	31
Figure 5.1. Schematic architectures of type A hyperbranched polymers of different molecular weights.	42
Figure 5.2. Configuration of type A hyperbranched polymers with different molecular weights in comparison with dendrimers and linear polymers.....	43

Figure 5.3. Schematic architectures of hyperbranched polymers of the same molecular weight of 187 beads but different number of spacers.	44
Figure 5.4. Configurations of hyperbranched polymers comprising 187 beads but with different number of spacers.....	45
Figure 5.5. Configuration of type A hyperbranched polymer with 187 monomers at strain rates of (a) 0.0001, (b) 0.001, (c) 0.01 and (d) 0.1.....	47
Figure 5.6. Mean squared radii of gyration of the type A hyperbranched polymers of different molecular weights at different strain rates.	49
Figure 5.7. Comparison of radii of gyration for type A hyperbranched polymers, dendrimers and linear polymers.	50
Figure 5.8. Dependence of the radius of gyration on strain rate for hyperbranched polymers with the same molecular weight of 187 beads but different numbers of spacers.	51
Figure 5.9. Dependence of zero shear rate radii of gyration on Wiener index for 187 bead hyperbranched polymers with different numbers of spacers (the solid line representing fitting with the exponential function).	52
Figure 5.10. Dependence of zero shear rate radii of gyration on the number of beads per molecule for type A hyperbranched polymers.	54
Figure 5.11. Dependence of the Wiener index on the number of beads per molecule for short branch hyperbranched polymers of type A.	54
Figure 5.12. Mean squared radii of gyration for blends of 187 bead linear polymers and hyperbranched polymers of (a) type A, (b) type D with different hyperbranched polymer fractions and (c) type A and D with hyperbranched polymer fraction of 20% and squared radii of gyration for pure 187 bead linear polymers.....	56
Figure 5.13. Averaged eigenvalues of the tensor of gyration for type A hyperbranched polymers of different molecular weights.	57
Figure 5.14. Ratios of averaged eigenvalues of the tensor of gyration for type A hyperbranched polymers with different molecular weights.....	59
Figure 5.15. Eigenvalues of the average tensor of gyration for type A hyperbranched polymers of different molecular weights.	60
Figure 5.16. Ratios of eigenvalues of the average tensor of gyration for type A hyperbranched polymers in comparison with those of dendrimers and linear polymers.	61
Figure 5.17. Distribution of beads from the core for type A hyperbranched polymers of different molecular weights at strain rates of (a) 0.0001, (b) 0.1 and (c) for type A hyperbranched polymers with 91 monomers at various strain rates.	63

Figure 5.18. Distribution of beads from the centre of mass for type A hyperbranched polymers of different molecular weights at strain rates of (a) 0.0001, (b) 0.1 and (c) for type A hyperbranched polymers with 91 monomers at various strain rates.....	64
Figure 5.19. Distribution of mass from the centre of mass for hyperbranched polymers of the same molecular weight of 187 beads but with different numbers of spacers (a) at strain rate of 0.0001, (b) at strain rate of 0.02 and (c) hyperbranched polymer of type B at strain rate of 0.0001 and 0.02.....	66
Figure 5.20. Distribution of mass from the core for hyperbranched polymers of the same molecular weight of 187 beads but with different numbers of spacers (a) at strain rate of 0.0001, (b) at strain rate of 0.02 and (c) hyperbranched polymer of type B at strain rate of 0.0001 and 0.02.....	67
Figure 5.21. Distribution of mass from the centre of mass for blends of 187 bead hyperbranched polymers and linear chains of equivalent weight at strain rate of 0.0001. (a) Blends with different fractions of type A hyperbranched polymers, (b) Blends with different fractions type D hyperbranched polymers and (c) Blends with 20% hyperbranched polymers of type A or D.	69
Figure 5.22. Distribution of terminal groups for type A hyperbranched polymers of different molecular weights at strain rates of (a) 0.0001, (b) 0.1 and (c) hyperbranched polymers with 91 beads at various strain rates.....	70
Figure 5.23. The atomic radial distribution function for 187 bead hyperbranched polymers with different numbers of spacers at the strain rate of 0.0001.	72
Figure 5.24. Atomic radial distribution function for blends of 187 bead linear polymers and hyperbranched polymers of (a) type A and (b) type D.....	73
Figure 5.25. Atomic radial distribution function for type A hyperbranched polymer with 91 beads at strain rates of 0.0001 and 0.1.	74
Figure 5.26. Interpenetration in the melts of type A hyperbranched polymers of different molecular weights at the strain rate of (a) 0.0001 and (b) 0.1.	75
Figure 5.27. Comparison of the interpenetration function for hyperbranched polymers of the same molecular weight of 187 beads but with different numbers of spacers (a) at strain rate of 0.0001, (b) at strain rate of 0.02 and (c) type A hyperbranched polymer at strain rate of 0.0001 and 0.02.....	76
Figure 5.28. Molecular alignment angle for hyperbranched polymers of (a) type A with different molecular weights and (b) different numbers of spacers.	78
Figure 5.29. Order parameter of the molecular alignment tensor for hyperbranched polymers of (a) type A with different molecular weights and (b) the same molecular weight of 187 beads but with different numbers of spacers.....	80
Figure 5.30. The eigenvalues of the molecular alignment tensor for hyperbranched polymers with the same molecular weight of 187 beads but different numbers of spacers.	81

Figure 5.31. Bond alignment angle for (a) linear polymers and (b) type A hyperbranched polymers of different molecular weights.....	83
Figure 5.32. Bond alignment angle for hyperbranched polymers with the same molecular weight of 187 beads but different numbers of spacers.....	84
Figure 5.33. Bond order parameter for (a) linear polymers and (b) type A hyperbranched polymers of different molecular weights.	85
Figure 5.34. Order parameter of the bond alignment tensors for hyperbranched polymers with the same molecular weight of 187 beads but different numbers of spacers at different strain rates.....	86
Figure 5.35. The eigenvalues of the bond alignment tensor for hyperbranched polymers with the same molecular weight of 187 beads different numbers of spacers.....	87
Figure 6.1. Dependence of shear viscosity on strain rate for type A hyperbranched polymers of different molecular weights (solid lines representing fitting with the Carreau-Yasuda model).	90
Figure 6.2. Carreau-Yasuda equation vs. Cross equation fitted for shear viscosity data for type A hyperbranched polymers composed of 187 monomers.	92
Figure 6.3. Zero shear viscosity vs. number of beads per molecule for hyperbranched polymers of type A.....	93
Figure 6.4. Longest relaxation time versus number of beads per molecule for type A hyperbranched polymers.	95
Figure 6.5. Dependence of the ratio η/η_0 on the Weissenberg number for type A hyperbranched polymers of different molecular weights.....	96
Figure 6.6. Shear viscosities versus strain rate for 187 bead hyperbranched polymers (a) of different types in <i>NVT</i> simulations, (b) of different types in <i>NpT</i> simulations and (c) of type A in <i>NVT</i> and <i>NpT</i> simulations (solid lines representing fitting with the Cross model).	97
Figure 6.7. Dependence of zero shear rate viscosities on the number of spacers for 187 bead hyperbranched polymers.....	99
Figure 6.8. Shear viscosities versus Weissenberg number calculated from the time constant of the Carreau-Yasuda model for 187 bead hyperbranched polymers with different numbers of spacers in <i>NVT</i> and <i>NpT</i> simulations (solid lines representing fitting with the Carreau-Yasuda model).....	101
Figure 6.9. Shear viscosities versus Weissenberg number calculated from the time constant of the Cross model for 187 bead hyperbranched polymers with different numbers of spacers in <i>NVT</i> and <i>NpT</i> simulations (solid lines representing fitting with the Cross model).	102
Figure 6.10. Shear viscosity of blends of hyperbranched and linear polymers composed of 187 beads per molecule at different strain rates. (a) Hyperbranched polymer of	

type A with different blend proportions. (b) Hyperbranched polymer of type D with different blend proportions. (solid lines representing fitting with the Carreau – Yasuda equation) (c) Hyperbranched polymers of type A and D with the blend proportion of 20%.	107
Figure 6.11. Comparison of shear viscosity for pure 187 bead hyperbranched polymer of type A, pure 187 bead linear chain and the blend of these polymers with the hyperbranched polymer fraction of 20%.....	107
Figure 6.12. Shear viscosity versus hyperbranched polymer fractions for blends of (a) type A and (b) type D hyperbranched polymers and linear chains of equivalent molecular weight of 187 beads at different strain rates.	108
Figure 6.13. First and second normal stress coefficients versus strain rate for type A hyperbranched polymers of different molecular weights.....	111
Figure 6.14. Ratio of the second and first normal stress coefficients for type A hyperbranched polymers of different molecular weights.....	112
Figure 6.15. First normal stress coefficient versus strain rate for 187 bead hyperbranched polymers (a) with different numbers of spacers in <i>NVT</i> simulations, (b) with different numbers of spacers in <i>NpT</i> simulation and (c) of type A in <i>NVT</i> and <i>NpT</i> simulations.....	114
Figure 6.16. Second normal stress coefficient versus strain rate for 187 bead hyperbranched polymers (a) with different numbers of spacers in <i>NVT</i> simulations, (b) with different numbers of spacers in <i>NpT</i> simulation and (c) of type A in <i>NVT</i> and <i>NpT</i> simulations.....	115
Figure 6.17. First normal stress coefficients of blends of hyperbranched and linear polymers composed of 187 beads per molecule at different strain rates.	117
Figure 6.18. Second normal stress coefficients of blends of hyperbranched and linear polymers composed of 187 beads per molecule at different strain rates.	118
Figure 6.19. Comparison of first normal stress coefficients for pure hyperbranched polymer of type A, pure linear chain and the blend of these polymers with the hyperbranched polymer fraction of 20% (all these polymers have the same molecular weight of 187 beads).	119
Figure 6.20. Dependence of the isotropic pressure on strain rate for type A hyperbranched polymers of different molecular weights (solid lines representing fitting with the Carreau-Yasuda model).....	120
Figure 6.21. Dependence of the (a) isotropic pressure and (b) reduced bead density on strain rate of 187 bead hyperbrached polymers with different numbers of spacers in <i>NVT</i> and <i>NpT</i> simulations respectively (solid lines representing fitting with the Carreau-Yasuda model).	122
Figure 6.22. Density of blends of 187 bead linear polymers and 187 bead hyperbranched polymers of (a) type A and (b) type D with different hyperbranched polymer proportions.	125

Figure 6.23. Deviations from the stress-optical rule $-(P_{xx} - P_{yy}) / (S_{xx} - S_{yy})$ and $(P_{yy} - P_{zz}) / (S_{yy} - S_{zz})$ versus $\dot{\gamma}$ for type A hyperbranched polymers of different molecular weights. 127

Figure 6.24. Deviations from the stress-optical rule $-(P_{xx} - P_{yy}) / (S_{xx} - S_{yy})$ and $(P_{yy} - P_{zz}) / (S_{yy} - S_{zz})$ versus $\dot{\gamma}$ for hyperbranched polymers with the same molecular weight of 187 beads but different numbers of spacers..... 129

List of Tables

Table 5.1. Degree of branching and Wiener index for hyperbranched polymers of the same molecular weight of 187 beads but with different number of spacers.....	46
Table 5.2. Zero shear rate radii of gyration for blends of 187 bead hyperbranched and linear polymers.....	55
Table 6.1. Parameters of the Carreau-Yasuda model fitted to the shear viscosity versus strain rate dependence of type A hyperbranched polymers.	91
Table 6.2. Parameters of the Cross equation fitted to the shear viscosity versus strain rate dependence for type A hyperbranched polymers.....	92
Table 6.3. Parameters of the Cross model fitted to the shear viscosity versus strain rate dependence for 187 bead hyperbranched polymers with different numbers of spacers.	98
Table 6.4. Parameters of the Carreau-Yasuda model fitted to the shear viscosity versus strain rate dependence for 187 bead hyperbranched polymers with different numbers of spacers.	100
Table 6.5. Carreau – Yasuda fitting parameters for shear viscosity data of blends of the type A hyperbranched polymers and linear chains of equivalent molecular weight of 187 beads.	106
Table 6.6. Carreau – Yasuda fitting parameters for shear viscosity data of blends of the type D hyperbranched polymers and linear chains of equivalent molecular weight of 187 beads.	106
Table 6.7. Cross fitting parameters for shear viscosity data of blends of type A hyperbranched polymers and linear chains of equivalent molecular weight of 187 beads.....	106
Table 6.8. Cross fitting parameters for shear viscosity data of blends of the type D hyperbranched polymers and linear chains of equivalent molecular weight of 187 beads.....	107
Table 6.9. Linear fitting parameters for shear viscosity data dependence on hyperbranched polymer fraction for blends comprising type A polymers composed of 187 beads per molecule.....	109
Table 6.10. Linear fitting parameters for shear viscosity data dependence on hyperbranched polymer fraction for blends comprising the type D polymers composed of 187 beads per molecule.	109
Table 6.11. Estimated values of the exponents in the power-law regions for the first and second normal stress coefficients of type A hyperbranched polymers.....	112

Table 6.12. Estimated values of the exponents in the power law regions for the first and second normal stress coefficients of 187 bead hyperbranched polymers with different numbers of spacers.	113
Table 6.13. Parameters of the Carreau-Yasuda model fitted to the isotropic pressure versus strain rate dependence for hyperbranched polymers with the same molecular weight of 187 beads but different numbers of spacers.....	123
Table 6.14. Parameters of the Carreau-Yasuda model fitted to the reduced bead density versus strain rate dependence for hyperbranched polymers with the same molecular weight of 187 beads but different numbers of spacers.....	123
Table 6.15. Zero shear rate density for blends of 187 bead hyperbranched and 187 bead linear polymers with different hyperbranched polymer fractions.....	124

Notation

Abbreviations

FENE	Finitely Extensible Nonlinear Elastic potential
LJ	Lennard-Jones potential
MD	Molecular Dynamics
NEMD	Non-Equilibrium Molecular Dynamics
WCA	Weeks-Chandler-Anderson potential

Latin alphabet

b	<i>spacer</i> – number of beads in a linear unit of a dendritic polymer
B	degree of branching
d_{ij}	number of bonds separating site/bead i and j of a molecule
D	number of fully branched units in a hyperbranched molecule
\mathbf{D}	rate of strain tensor
f	functionality of the branch groups of a dendritic polymer
f_c	functionality of the core of a dendritic polymer
\mathbf{F}_i	force acting on molecule i
$\mathbf{F}_{i\alpha}$	force acting on bead α in molecule i
$\mathbf{F}_{i\alpha j\beta}$	intermolecular force on bead α in molecule i due to bead β in molecule j
g	generation number of a dendrimer
$g_A(r)$	atomic radial distribution function
$g_{CM}(r)$	distribution of beads from the centre of mass
$g_{core}(r)$	distribution of beads from the core
$g_{inter}(r)$	interpenetration function
$g_{term}(r)$	radial distribution of terminal group
\mathbf{I}	tensor of inertia, unit tensor
k	spring constant of the FENE potential
k_B	Boltzmann constant
K	consistency index in the Cross model

l_{bond}	bond length
L	number of partially reacted units in a hyperbranched molecule
L_y	size of the simulation box along the y axis
L_1, L_2, L_3	mean eigenvalues of the tensor of gyration
L'_1, L'_2, L'_3	eigenvalues of the mean tensor of gyration
m	mass of a single bead
m_C	power law exponent in the Cross model fitted for shear viscosity data
m_p	power law exponent in the Carreau-Yasuda model fitted to isotropic pressure data
m_ρ	power law exponent in the Carreau-Yasuda model fitted to reduced bead density
M	mass of a molecule
N	number of molecules
N_s	number of beads composing a single molecule
N_t	total number of beads composing the system
N_1	first normal stress difference
N_2	second normal stress difference
p	isotropic pressure
p_η	power law exponent in the Carreau-Yasuda model fitted for shear viscosity data
p_{R_g}	power law exponent in the Carreau-Yasuda model fitted to radius of gyration data
\mathbf{P}	pressure tensor
\mathbf{P}^A	atomic pressure tensor
\mathbf{P}^M	molecular pressure tensor
P_{xy}	xy element of the pressure tensor
\mathbf{p}_i	momentum of the centre of mass of molecule i
$\mathbf{p}_{i\alpha}$	momentum of bead α in molecule i
Q	damping factor in the NpT algorithm

\mathbf{r}_i	position of the centre of mass molecule i
\mathbf{r}_α	position of bead α
$\mathbf{r}_{i\alpha}$	position of bead α in molecule i
\mathbf{r}_{CM}	position of the centre of mass
\mathbf{r}_{i1}	position of the core of molecule i
r_{ij}	distance between centres of mass of molecule i and molecule j
R_0	finite extensibility of the FENE spring
\mathbf{R}_g^2	tensor of gyration
$\langle R_g^2 \rangle$	mean squared radius of gyration
$\langle R_g^2 \rangle_0$	zero shear rate mean squared radius of gyration
R_g	radius of gyration
\mathbf{S}_m	molecular alignment tensor
\mathbf{S}_b	bond alignment tensor
S_m	molecular order parameter
S_b	bond order parameter
$S_{m,i}$	eigenvalue of the molecular alignment tensor
$S_{b,i}$	eigenvalue of the bond alignment tensor
S_{xx}	xx component of the alignment tensor
Δt	integration time step
T	temperature
$u_x(t)$	x component of the streaming velocity vector
\mathbf{u}_i	unit vector denoting the orientation of molecule i
\mathbf{v}_i	unit vector denoting the orientation of bond i
U	interaction potential energy
U_{ij}^{FENE}	FENE interaction energy between beads i and j
U_{ij}^{LJ}	LJ interaction energy between beads i and j
U_{ij}^{WCA}	WCA interaction energy between beads i and j
V	volume of the simulation box

W	Wiener index
Wi	Weissenberg number

Greek alphabet

α	power law exponent for first normal stress coefficients
β	power law exponent for second normal stress coefficients
$\dot{\gamma}$	shear rate
$\dot{\gamma}_c$	shear rate of the onset of shear thinning
ε	LJ energy parameter
$\dot{\varepsilon}_{xx}$	compression rate along x axis
η	shear viscosity in the steady shear
η_0	zero shear viscosity
η_∞	infinite shear viscosity
$[\eta]$	intrinsic viscosity
κ	characteristic strain rate in the flow
λ	characteristic time of the fluid
λ_η	time constant in the Carreau-Yasuda model fitted for shear viscosity data
λ_p	time constant in the Carreau-Yasuda model fitted for isotropic pressure data
λ_ρ	time constant in the Carreau-Yasuda model fitted for reduced bead density data
λ_{R_g}	time constant in the Carreau-Yasuda model fitted for radius of gyration data
ρ	bead concentration/density
$\boldsymbol{\sigma}$	stress tensor
σ	LJ length parameter
ζ	thermostatting coefficient
τ_0	longest relaxation time
χ_m	molecular alignment angle

χ_b	bond alignment angle
ψ_1	first normal stress coefficient
ψ_2	second normal stress coefficient